

# CHAPTER 176

## THE IN SITU MEASUREMENTS OF SEDIMENT TRANSPORT AND BOTTOM TOPOGRAPHY CHANGES

by

Yoshiaki KAWATA<sup>1</sup> M.ASCE, Hiroshi YOSHIOKA<sup>2</sup>  
and Yoshito TSUCHIYA<sup>3</sup> M.ASCE

### Abstract

In order to get the data about bed-load transport rate and bottom topography changes under storm wave conditions, field equipments were newly developed and tested at the T-shaped Observation Pier(TOP) on the Ogata coast facing the Japan Sea. The surf sled with a pressure sensor can precisely detect the spatial water depth changes along the survey lines. Based on the compiled data, the 3D bottom topography changes for a winter season connect with the appearance of a dip and shoal system on the Ogata coast. The bed-load sampler has also developed to operate in rough sea state in a plane bed conditions. The data were well fitted with the law of cross-shore bed-load transport proposed by Kawata(1989a).

### 1. INTRODUCTION

A meaningful field study of nearshore sediment dynamics requires the in situ measurement of sediment transport and bottom topography changes. The validity of various proposed sediment transport relationships by waves has not been evaluated in the field. For lack of extensive 3D bottom topography data under severe wave conditions, the reliability of any analytical and numerical prediction methods of beach processes is still ambiguous. Recent field observations such as NSTS program(Seymour, 1987), C<sup>2</sup>S<sup>2</sup>(Willis,1987) and Duck85(Mason et al.

---

<sup>1</sup>Associate Professor, Disaster Prevention Research Institute,  
Kyoto University, Goka-sho, Uji, Kyoto, 611 Japan

<sup>2</sup>Instructor

<sup>3</sup>Professor

1987) had been carried out but no one did not directly measure these variables. In our field study, simultaneous measurements were also made of waves, water particle motion and nearshore currents at various locations along the T-shaped Observation Pier(TOP) in the surf zone.

In the field, the rate of sediment transport normal to the beach has been measured with a newly developed bed-load trap in a series of field experiments conducted at the TOP. The law of sediment transport formulated by Kawata(1989a) can be verified with the field and experimental data. At the same time, a sounding method in rough sea state around the TOP has been also developed to discuss the beach processes on the Ogata coast.

## 2. PROCEDURE

The field experiments were conducted in the three winter seasons in 1988,1989 and 1990, the periods that encompass the more intense wave activity on the Ogata coast which is a straight sandy beach of 20km long facing the Japan Sea as shown in Fig.1. The TOP extends 250m offshore and parallels the shore for 100m at the offshore end. Usually, seven ultrasonic type wave gauges (aerial emission type) and one 2D and two 3D ultrasonic type current meters are installed for routine observation. In addition, intensive observation uses extra two 3D ultrasonic type current meters whose spacing is 1m in the vertical direction and ten capacitance

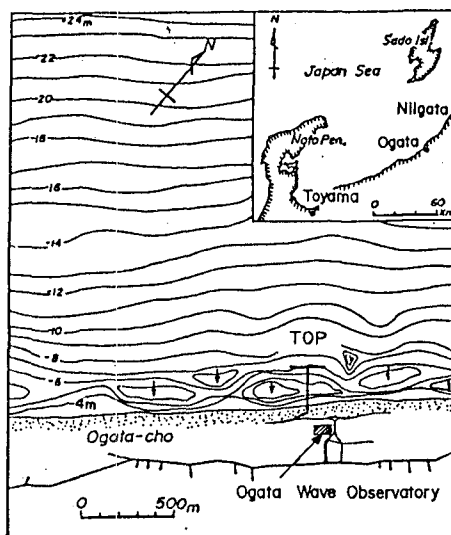


Fig.1 Locations of the Ogata coasts and T-shaped Observation Pier(TOP)

type wave gauges as shown in Fig.2. A wave-rider buoy is anchored at the 3km offshore. The buoy is on a production of the pier axis(almost NW direction) so that in the case of normal incident waves, wave transformation can be analyzed accurately. The nearshore zone in which the water depth is more than about 4m has a very mild slope of around 1/120. At the offshore end of the pier, the water depth is about 6m. All data are gathered and compiled at Ogata Wave Observatory.

2.1 Bed-load trap

The unique design of a bed-load trap has been evolved over several years. Some operation and setting problems had been solved one by one with some ideas. The trap can operate under moderate to severe wave conditions because it is installed by using the local scour around the trap itself. Photo 1 shows the shape, attached equipments and size. Before the setting of the trap on the sea bottom, the sand bed condition is confirmed to be the plane bed with a measuring comb of 1.8m long with 61 stings which are coated with the grease as shown in Photo 2. The small scale bottom undulations in the cross-shore direction can be measured.

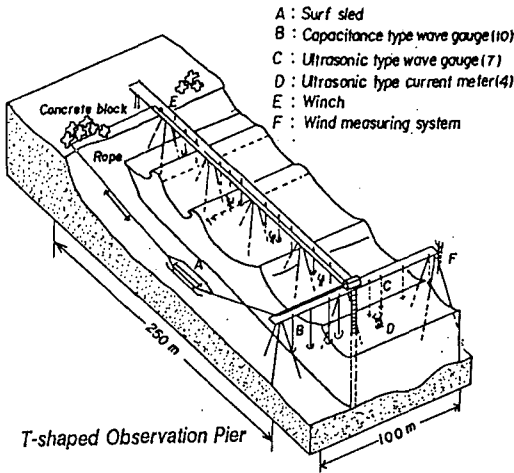


Fig.2 TOP and setting of surf sled, wave gauges, current meters and other equipments

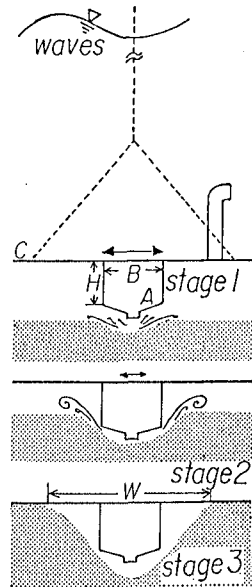
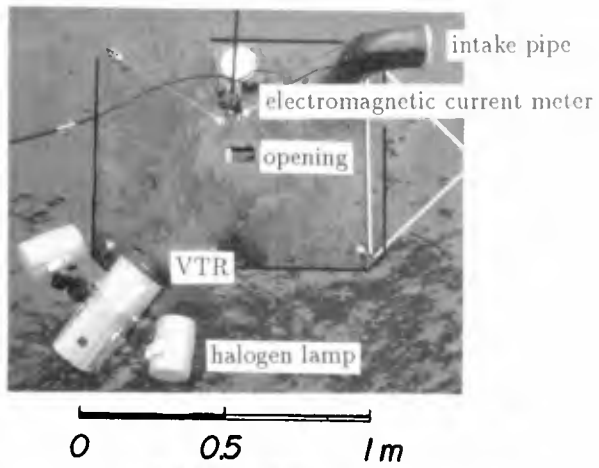


Fig.3 Procedure of setting of bed-load trap using local scouring



(a) Plane view



(b) Side view

Photo 1 Bed-load trap

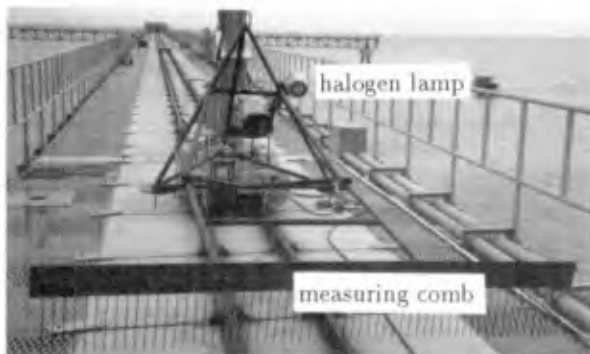


Photo 2 Measuring apparatus of small scale bottom undulations

Usually, at the breaker zone the plane bed condition is observed.

Fig.3 shows the setting process of the trap. Firstly, the opening(10cmx5cm) on the top steel plate of the trap is capped with a small cover which is fixed on the trap with an adhesive tape. This cover can be easily removed from the deck of the pier by pulling a fine string. Secondly, the trap is taken down into the sea by a crane and the air inside the trap is released through the intake pipe. Thirdly, the trap is touched on the bottom. The next moment local scouring around the trap advances. At the stage 3 in Fig.3, the trap is gradually stabilized in accordance with the development of the local scouring. The measurement of the bed-load transport starts in a moment when the string removes the cover from the opening of the trap. A compact videocassette recorder and two components electromagnetic current meter (the probe is set at the height of 17.3cm from the top plate of the trap) were equipped on the trap.

The net onshore (or offshore)bed-load transport rate can be just trapped through the opening on the plate. The inflow and outflow of sea water through the opening connected with a pipe as shown in Photo 1 keeps the one-way bed-load measurement. This system surely corresponds to the periodic changes of flow direction of water particle motion.

## 2.2 Surf sled

A surf sled (1.5m long, 0.7m wide, 40kg in weight) with a semiconductor pressure transducer has been also developed as shown in Photo 3. The sled can be operated in the cross-shore direction by two winches and roop rope system. The A-D converted data are compiled in the datalogger in a watertight stainless housing. With the sled the beach profiles were measured at longshore intervals of 5m. The sampling interval is 2.5s and average moving speed of the sled is 19.4cm/s. The overall error of the sounding keeps less than 5cm in any sea state. Preliminary tests show that low pass filter of 0.03Hz is adequate to eliminate the effect of incoming waves.



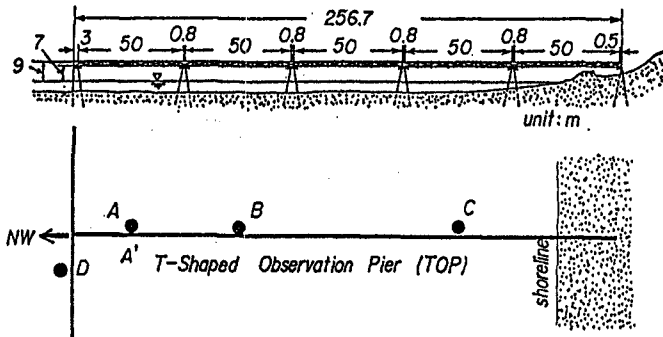
Photo 3 Surf sled

3. FIELD MEASUREMENTS

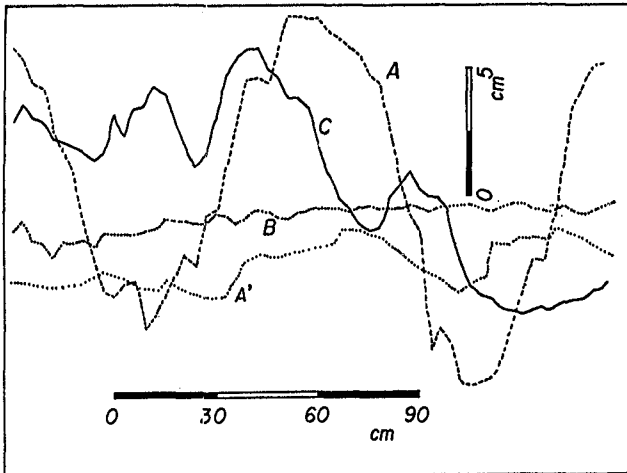
3.1 Bed-load transport

Fig.4 shows the sea bottom conditions at some measuring sites. In the surf zone on the Ogata coast, the rippled bed is usually observed and at the breaker zone, a plane bed condition is formed.

Fig.5 shows the cumulative curves of sediment on the bed and in the trap at site B. The mean diameters of the bed and of trapped sediment are 0.25mm and 0.3mm respectively. It was found that the relatively coarse part of the bed sediment moves as bed-load and therefore the standard deviation of the trapped sediment is smaller than that of the bed one.



(a) Measuring site around the pier



(b) Bottom conditions

Fig.4 Small scale bottom topography

Table 1 lists the results of observations on onshore sediment transport rate. These data are plotted in Fig.6 in which  $q_* (=q/u_* d)$  is dimensionless sediment transport rate and  $\tau_*$  is dimensionless tractive force (the Shields number). In the arrangement, some unknown variables were estimated with the small amplitude wave theory and the friction factors introduced by Jonsson (1966). The visual observation with a VTR shows that bed-load movement on the plate of the trap was very smooth and made a parallel stripe pattern of accumulated sediment on the plate of the trap in the cross-shore direction. When the direction of water particle motion changes to offshore, the discharge from the opening through the pipe can blow off sediment which usually falls into the trap as offshore sediment transport rate. Therefore, it was confirmed that the trap efficiency of onshore sand transport is very high. The solid line in the figure shows the theoretical relationship of cross-shore sediment transport rate given by Kawata (1989a) as follows:

The theoretical reduction for cross-shore sediment transport is based on the momentum conservation of a cloud of saltating sand particles on a sloping beach.

(a) In the case of onshore sediment transport

$$\begin{aligned}
 q_{*u} &= a_1 [1 + e + (1 - e) \sqrt{\sin \theta} / (\sqrt{3} / 2 A_r \sqrt{C_D \tau_*}) \\
 &\quad - \{1 - e + (1 + e) \sqrt{\sin \theta} / (\sqrt{3} / 2 A_r \sqrt{C_D \tau_*})\}^2 \\
 &\quad + 8(1 - e) \cos^2 \theta / (3 \lambda C_D A_r^2 \tau_*^2)^{1/2}] (\tau_* - \tau_{*c}) \quad \text{--- (1)}
 \end{aligned}$$

(b) In the case of offshore sediment transport

$$\begin{aligned}
 q_{*d} &= a_1 [1 + e - ((1 - e)^2 + 8 \cos^2 (1 - e - 2e \lambda \tan \theta) \\
 &\quad / (3 \lambda C_D A_r^2 \tau_*^2)^{1/2}] (\tau_* - \tau_{*c}) \quad \text{--- (2)}
 \end{aligned}$$

$$a_1 = (e/1 - 1) \tan \beta_m (1 + \rho/\sigma) A_r / \sqrt{\cos \theta}$$

$$\tau_{*c} = \tau_{*o} \{ \cos \theta \pm (\sigma/\rho) / (\sigma/\rho - 1) (\sin \theta / \tan \varphi) \}$$

Table 1 Results of field observation on onshore bed-load transport rate

No.	H <sub>1/3</sub> (m)	T <sub>1/3</sub> (s)	H <sub>m</sub> (m)	T <sub>m</sub> (s)	u <sub>1/3</sub> (cm/s)	u <sub>m</sub> * (cm/s)	t (s)	q** (cm <sup>3</sup> /cm/s)
1	1.38	5.41	0.88	4.51	-	-	658	9.48x10 <sup>-3</sup>
2	1.71	6.00	1.00	4.86	-	-	1583	69.8
3	0.94	4.65	0.63	3.97	58.5 (47.7)	34.6 (27.6)	1476	0.952
4	1.09	4.48	0.71	3.71	47.7 (52.5)	27.3 (37.5)	1554	2.18
5	1.00	4.43	0.68	3.87	-	-	1440	0.466
6	1.13	4.47	0.76	4.20	65.8 (52.0)	40.2 (30.2)	4967	1.03
7	0.88	4.82	0.61	4.07	50.3 (56.8)	26.5 (33.2)	1477	2.82
8	0.93	4.40	0.67	4.27	58.5 (64.0)	26.9 (46.0)	2398	7.36
9	1.10	4.98	0.75	4.38	41.7 (62.3)	23.7 (39.6)	1410	2.26
10	1.04	4.66	0.75	4.45	46.0 (64.0)	23.9 (44.3)	1366	1.73
11	1.59	4.94	1.07	4.93	72.6 (81.2)	43.9 (51.6)	1800	7.84
12	3.04	8.80	1.78	6.20	-	-	4360	36.8
13	1.98	4.40	1.26	3.00	-	-	4500	14.8

\* Parenthesis means offshore direction.

\*\* Substance volume (porosity is assumed to be 0.4)



in which  $\theta$ :beach slope,  $e$ :rebound coefficient of sand particle ,  $C_D$ :drag coefficient,  $A_r=8.5$ ,  $\lambda/4$ :ratio of height to length of a saltating sand particle,  $\sigma$  and  $\rho$ :densities of sand and fluid respectively,  $\varphi$ :angle of repose,  $\tau_*$ :the Shields number and suffix  $u$ ,  $d$  and  $c$ :upward slope, downward slope and critical condition respectively.

Typical variables are shown in Fig.6, in which the experiments of saltation of a sand particle were done in a water stream. In the horizontal bed, Eqs.(1) and (2) completely coincide. It should be noted that the trend of the field data calculated with mean wave height and period as well as experimental data in a plane bed condition is in reasonable agreement with the theory. However, arrangement with characteristics of significant waves is not adequate.

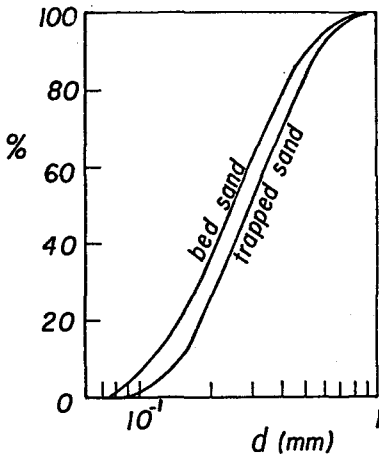


Fig.5 Sieve analysis of sediment

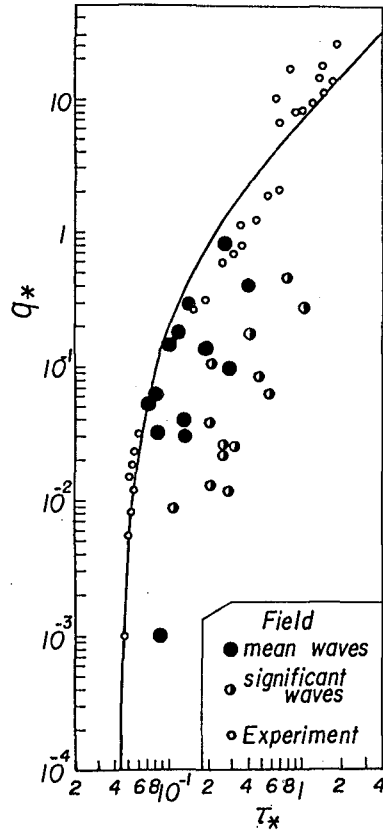


Fig.6 Relationship between the Shields number and dimensionless onshore sediment transport rate

### 3.2 Bottom topography changes

#### (1) Wave characteristics

The intensive observation was conducted from November 28 to December 7, 1987. In this period, some storms came on the Ogata coast. Fig.7 shows the time series of wave climate recorded by a wave-rider buoy, a capacitance type wave gauge at the east end of the pier. The wave directions were analyzed with the linear array of four capacitance type wave gauges at the offshore end. The water depth of about 6m at the offshore end of the pier controls the maximum wave height. The tidal range is less 40cm. Usually, low pressures move eastwards in the midst of the Japan Sea in winter season, so that wave directions change from west to east at the offshore. However, in the records of the wave directions at the pier, they are not widely distributed but have a sharp peak around  $90^\circ$  (This means that wave angles at the pier are perpendicular to the beach) as shown in Fig.8. In the peak, wind waves from WNW to NW and swell waves from NW to NNW are included. This results reveals that the longshore sediment transport in the coast is small in spite of a straight sandy beach.

#### (2) Erosion and deposition area

Fig.9 shows the bottom topography on December 9 and 10, 1987 and March 13, 1988 in which D and S depict dip and shoal respectively. Over this period, waves are usually very small, so that it is assumed that the bottom topography is not remarkably changed in other seasons except by typhoon. Firstly, it was pointed out from Fig.9(a) that the contour lines in the shallow area which is less than 4m are parallel each other, two shoals are appeared at the both offshore ends of the pier and a dip with the maximum water depth of 5.2m expands to the central zone of the pier. In Fig.9(b), it was found that the distance of two shoals becomes short and the dip further extends to west direction(upper side of the figure). In general, water depth around the pier increased after winter season. This is partly due to forced offshore sediment transport. The armour unit mounted in the foreshore reflects the incoming waves and makes this coast an wave energy reflected beach defined by Short(1979).

The erosion and deposition diagram as shown in Fig.10 was made from the bottom topography changes between two observation date. In the figure, a hatched line is a boundary between erosion and deposition areas. As the characteristics of bottom topography change, the areas of erosion and deposition are not uniformly distributed in the cross-shore direction. Moreover, the positions of dips and shoals are almost fixed around the pier. Fig.11 shows the depth sounding chart in July 1986 and 1987 around the pier and Fig.12 reveals the pattern of dip and shoal in another place on the Ogata coast(kawata, 1989b). The distribution

pattern of dip and shoal was not changed annually, so that this system is stable and crescentic bars are formed on the Ogata coast. As before mentioned, there are two dominant wave directions on the Ogata coast. Their breaking points are usually a little different in the offshore direction, i.e., the fully-developed wind waves break relatively offshore in comparison with the breaking of the swell waves. Moreover, their incoming angles are slightly different. This characteristics may introduce the typical crescentic bar systems.

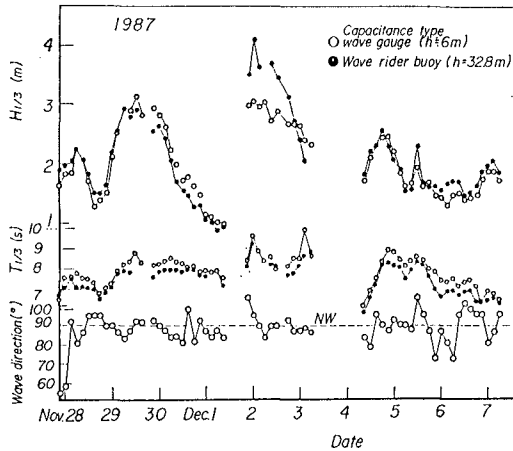


Fig.7 Changes of significant wave height and period and wave direction

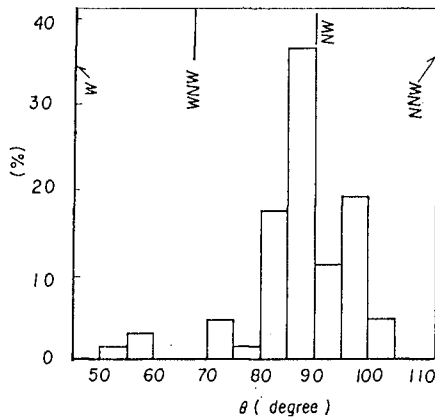
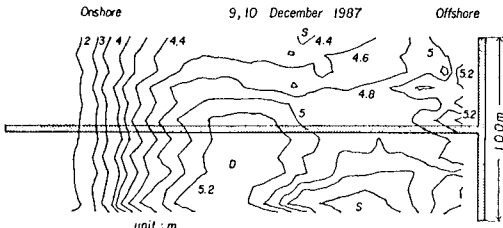
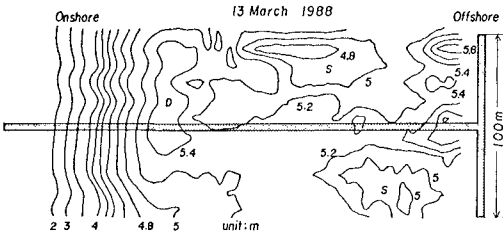


Fig.8 Histogram of incident wave angles at the offshore end of the TOP



(a) 9 and 10 December 1987



(b) 13 March 1988

Fig.9 bottom topography around the TOP

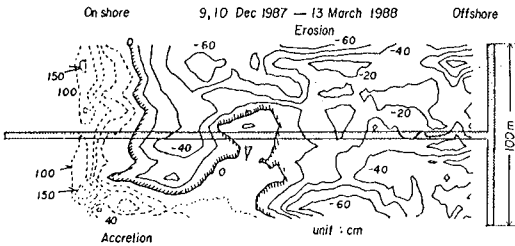


Fig.10 Deposition and erosion diagram

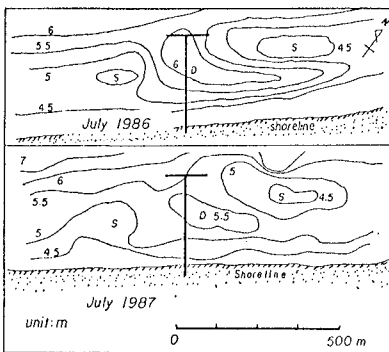


Fig.11 Depth sounding charts in Summer

(3) Beach profile changes

Along the pier the depth sounding with a lead has been conducted every week. The sounding interval in the cross-shore and longshore directions is 1.25m. The width of the pier is 4m so that we have two set of data along the pier in the cross-shore direction. The discrepancy of the mean beach profiles is very small so that the west side data were used in the analysis. The temporal difference from the mean beach profile are shown in Fig.13 in which black and grey areas show erosion and accretion from the mean beach profile respectively. In early winter, the offshore area beyond  $x=70m$  was eroded, but this tendency was gradually eliminated and finally the deposition area was appeared. As shown in Fig.9,

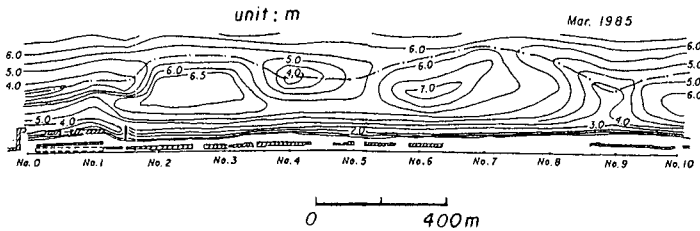


Fig.12 Typical bottom topography changes on the Ogata coast

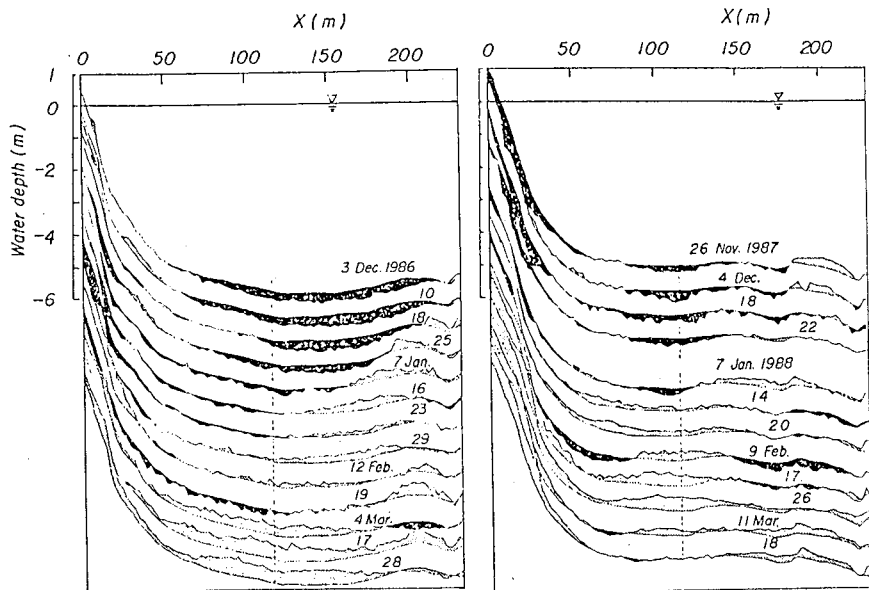


Fig.13 Beach profile changes in winter

this area is a "battle" zone of accretion and deposition areas. It is explained that westward longshore sediment transport may contribute the deposition in this area in winter season. From the data of the ultrasonic type current meter, strong undertow was observed around this place so that local changes of bottom topography may largely depend on the 3D nearshore current system.

#### 4. CONCLUSIONS

A new type bed-load trap has been developed with two ideas. The principles are as follows: local scouring around the trap stabilizes the trap itself and an intake pipe keeps the onshore or offshore sediment transport rate in the trap. The effectiveness of the trap was certified with VTR analysis under sheet flow conditions. The field data as well as experimental one on a plane bed confirmed the validity of the law of cross-shore sediment transport proposed by Kawata(1989).

A surf sled is also applicable to the measurement of bottom topography changes under rough sea state. The accurate sounding data can reveal the beach processes on the Ogata coast. This sandy straight beach has a series of crescentic bars which correspond to the dip and shoal system in the longshore direction. Under small longshore transport rate due to almost normal incoming waves, their positions are annually stable. The slight discrepancy of incoming wave angles between fully- developed wind waves and swell ones makes the direction of sediment transport complex and may lead to formation of the crescentic bar systems.

#### REFERENCES

- Jonsson, I. G. (1966): Wave boundary layer and friction factor, Proc. 10th ICCE, pp. 127-148.
- Kawata, Y. (1989a): The law of cross-shore sediment transport, Proc. Coastal Engineering, JSCE, Vol. 36, pp. 289-293.
- Kawata, Y. (1989b): Methodology of beach erosion control and its application, Coastal Engineering in Japan, Vol. 32, No. 1, pp. 113-132
- Mason C., W. A. Birkemeier and P.A. Howd (1987): Overview of DUCK85 near-shore processes experiment, Coastal Sediments '87, pp. 818-833.
- Seymour, R. J. (1987): An assessment of NSTS, Coastal Sediments '87, pp. 642-651.
- Short, A. D. (1979): Three-dimensional beach-stage model, J. Geology, Vol. 87, pp. 553-571.
- Willis, D. H. (1987): The Canadian coastal sediment study: an overview, Coastal Sediments '87, pp. 682-693.